이학석사학위논문

Single Molecule FRET Studies on Mph1

단일분자 FRET 방법을 이용한 Mph1 단백질 연구

2014 년 2 월

서울대학교 대학원
물리천문학부
박 정 빈

Single Molecule FRET Studies on Mph1

지도교수 홍 성 철

이 논문을 이학석사 학위논문으로 제출함

2013년 11월

서울대학교 대학원

물리천문학부

박 정 빈

박정빈의 이학석사 학위논문을 인준함.

2013 년 12 월

위 원 장 홍 승 훈 (인)

부위원장 홍 성 철 (인)

위 원 강 병 남 (인)

Master′s thesis

Single Molecule FRET Studies on Mph1

Jeongbin Park

***Research Advisor*: Professor Sungchul Hohng**

February 2014

School of Physics and Astronomy

Seoul National University

Abstract

Mph1 from *Saccharomyces cerevisiae* is an ATP-dependent 3'-5' DNA helicase involved in DNA damage bypass. Similar to its human homologue FANCM (Fanconi anemia, complementation group M), the protein is involved in repairing DNA at stalled replication forks by inter-strand crosslinks (ICLs). Here, we studied the fork regression activity of Mph1 on replication forks by single-molecule FRET (Fluorescence resonance energy transfer). We found that formation of the chicken-foot structure, which indicates initiation of the fork regression, was closely correlated to unwinding of lagging strand. In addition to that, surprisingly, we observed that Mph1 moves back and forth when it meets non-homologous pair between the leading and lagging strands.

Keywords: Mph1, DEAH-box DNA helicases, DNA Replication, Fork Regression, Resolve of ICLs, smFRET

Student Number: 2012-20361

Table of Contents

Chapter 1

Single Molecule FRET Studies on Mph1

1. Introduction

In genetics, DNA inter-strand crosslinks (ICLs) [1] are formed by various reagents including natural products of metabolism, which react with two opposite strands of DNA to covalently link each other. Because the two strands are tightly linked together, helicases cannot unwind the linked DNA strands, which corresponds to blockage of DNA replication. Resolving of stalled replication fork is an important procedure of cell cycle; recovery failure even corresponds to cell death [2,3].

Human orthologue of Mph1, FANCM (Fanconi anemia, complementation group M) is known as involved in recognizing [4] and resolving ICLs [5], by remodels it into chicken foot structure [6]. Then the fork is stabilized by the Fanconi anemia (FA) pathway, but still lots of questions are remain on the ICL repair process.

It is also believed that *Saccharomyces Cerevisiae* Mph1 [7,8] takes part of ICL

recovery process [9,10]. Similar to FA repair pathway, Mph1 promotes fork regression of ICL stalled replication fork, and then Exo1 and Slx4 (FANCP) restore ICL.

Fork regression activity of Mph1 is observed quantitatively by gel electrophoresis experiments [11], but still no single-molecule experiment was performed. Here, single molecule FRET (smFRET) experiments were performed to investigate the fork regression activity of Mph1.

2. Experimental Scheme

To investigate fork regression activity of Mph1, single molecule FRET (smFRET) experiment is performed. Figure 1 shows the experimental scheme of smFRET. DNA replication fork sample was immobilized to the surface of quartz slide by streptavidin-biotin interaction. Prism-type TIRF microscopy was used for selective visualization of surface of quartz slide, also for getting high quality single molecule images [12]. In this figure, Cy3 (green circle) and Cy5 (red circle) was attached to the DNA sample. The injected Mph1 molecules are drawn as blue rectangles. The detail methods are described in the Method section below.

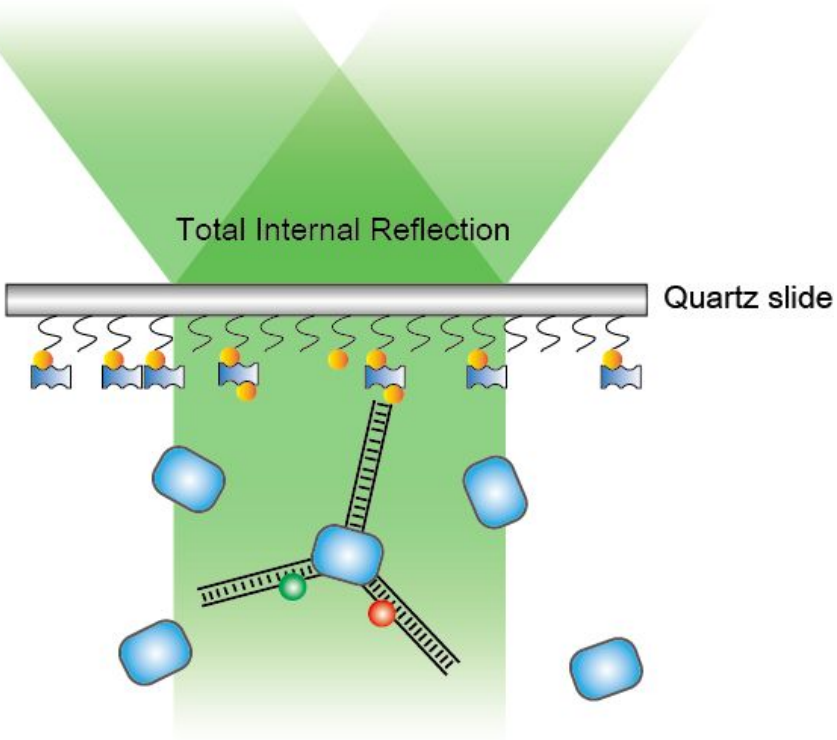

Figure 1

Single molecule FRET experimental scheme to observe fork regression activity of Mph1. Evanescent wave from total internal reflection excites DNA attached Cy3 and Cy5. The DNA samples are attached on surface by avidin-biotin interaction. The injected Mph1 proteins are drawn as blue rectangles.

3. Results

3.1. Fork Regression

The Cy3 and Cy5 dyes were labeled to the daughter strands of the fork sample to observe fork regression. Before Mph1 binds to the fork sample, the distance between Cy3 and Cy5 dyes are relatively long, so the FRET efficiency is low. But when Mph1 binds to the sample and starts regression, the distance between the dyes become close and the FRET is high. After fork regression, finally, the daughter strands are dissociated out then no fluorescence signal is observed (Figure 2).

Figure 3a shows the single-molecule fluorescence intensity trace for each dye. Alternating laser excitation (ALEX) method was used for monitor both Cy3 and Cy5 signal simultaneously, to observe dissociation of daughter strands. The upper trace shows that the excitation of Cy3 by 532 nm laser, the lower trace shows that the direct excitation of Cy5 by 633 nm laser. When the daughter strands were dissociated out, the Cy3 and Cy5 signals are disappeared simultaneously; although each dye can bleached out, but the probability of bleaching at the same time is really low – so the simultaneous disappearing of two dye signals can be considered as the dissociation event. The fork regression time, τ_d, was measured (Figure 3a).

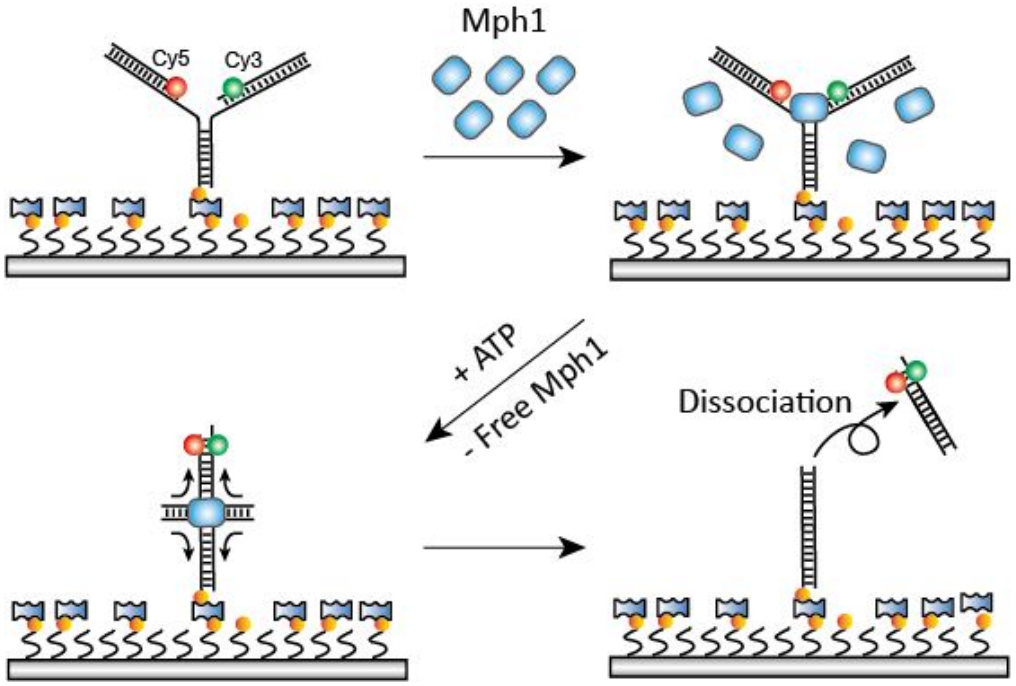

Figure 2

Fork regression by Mph1. Mph1 is represented as blue rectangle. Before initiation of fork regression, displacement and annealing of two daughter strands occurs. When the daughter strands are fully regressed back, the annealed daughter strands dissociated out from the parent strand.

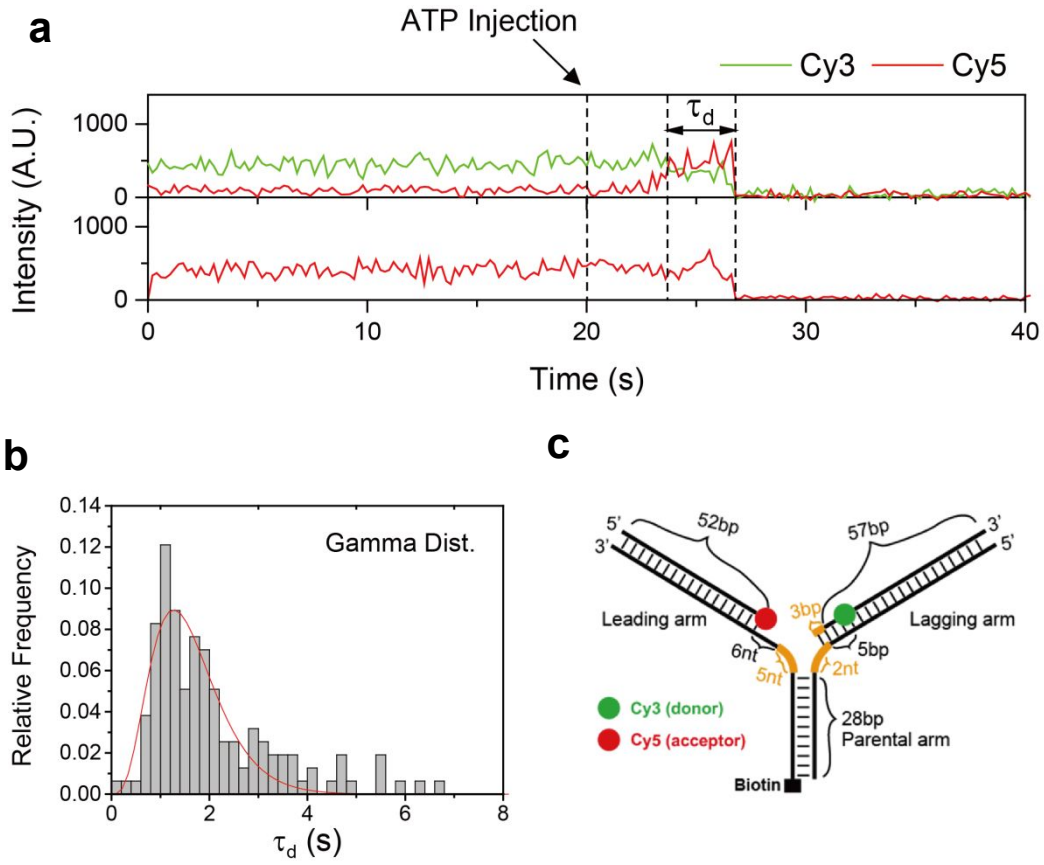

Figure 2

a) Representative single-molecule trace of fork regression by Mph1. The upper window indicates green laser (532 nm) excitation; the lower one indicates red laser (633 nm) excitation. The green and red line indicates the Cy3 and Cy5 signal, respectively. The time between the initiation of fork regression (FRET efficiency is 0.5) and the end of fork regression, τ_d, was measured.

b) Distribution of τ_d. Red line indicates the fitted curve to the gamma distribution function.

c) DNA sample used to the experiment. Cy3 and Cy5 were attached on the junction side of the sample.

The distribution of fork regression time shows gamma distribution, which means that the fork regression of Mph1 occurs through several steps (Figure 3b).

3.2. Measuring Regression Speed

Moreover, the length of arm side of fork sample is varied to measure the regression speed of Mph1 (Figure 3). To measure average speed of regression, several hundreds of base-pairs arm length of DNA sample was tested. The tested arm lengths were N=0, 150, and 319 bp. The average regression speed was calculated as the reciprocal of the slope of the linear fitted line to the τ_d vs. N graph. The calculated regression speed was 1.2bp/sec, which looks like opposite result from the gamma distribution of Figure 2. But the distribution of Figure 2 also shows thick tail after the 4 seconds of τ_d, so taking the arithmetic average of the τ_d would not give correct speed of the regression. Further studies are required for explaining the difference of results.

3.3. Before Regression

The waiting time between ATP injection and initiation of fork regression, τ_f, was also measured. The distribution of the time shows clear single exponential distribution (Figure 4b), which implies that one big rate-limiting step dominates the

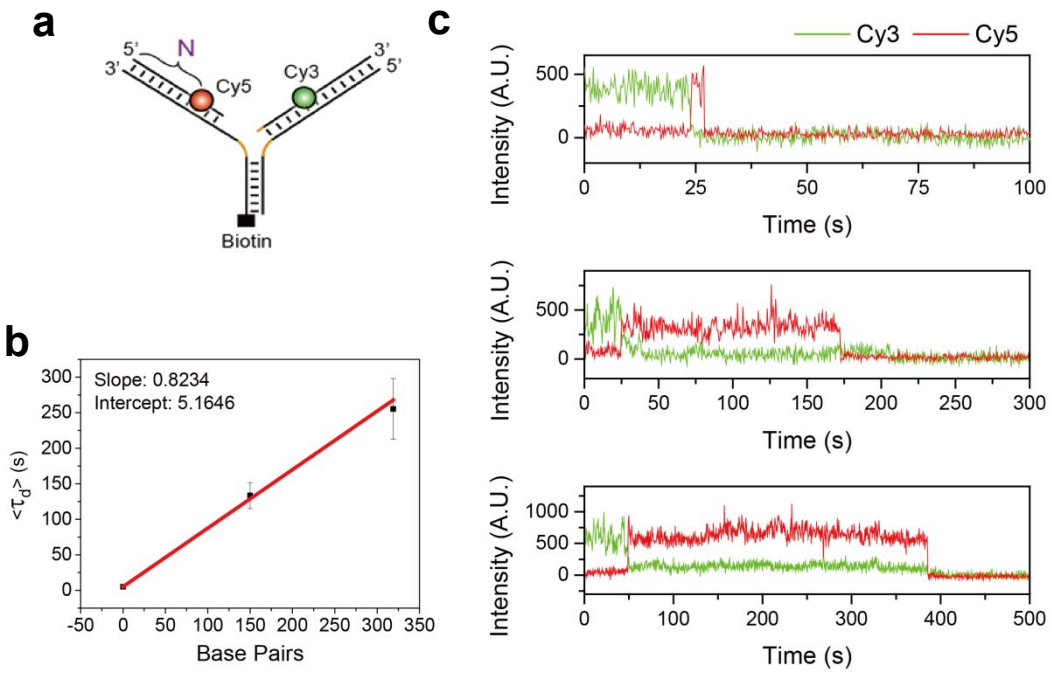

Figure 3

a) DNA sample design to measure regression speed of Mph1. Tested cases of N were 0, 150, and 319 bp.

b) τ_d vs N (Base pairs) graph. The red line indicates linear fit of the three data points. The slope and intercept was indicated inside the graph.

c) Representative traces of each N case. The measured τ_d was increased along the N increases.

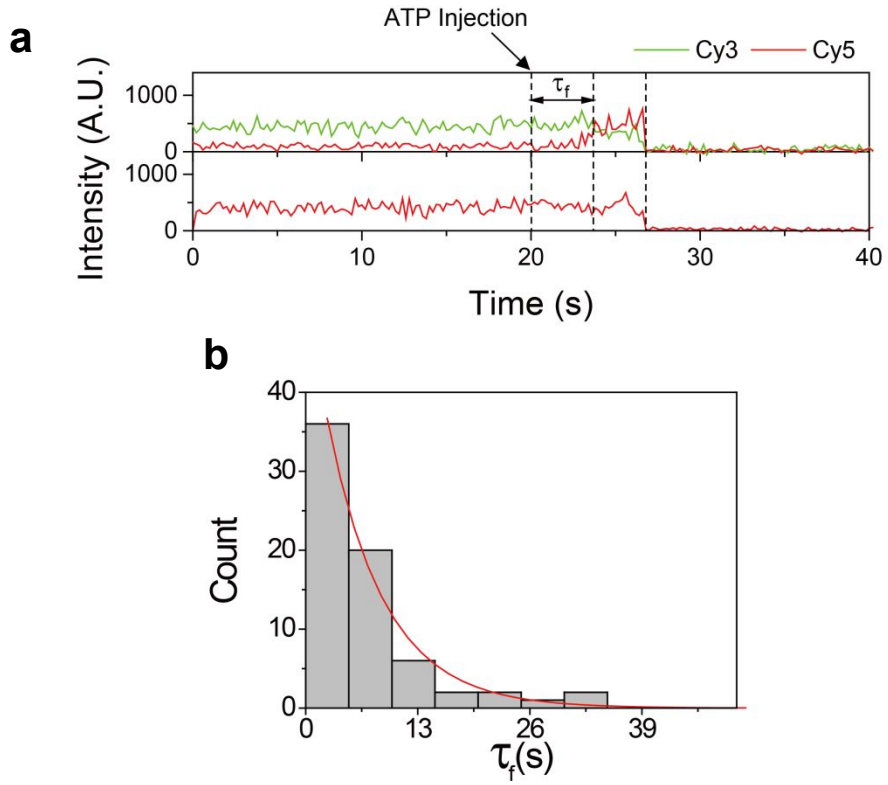

Figure 4

a) Representative single-molecule trace of fork regression by Mph1. The time between the injection of ATP and the initiation of fork regression (FRET efficiency is 0.5), τ_f, was measured.

b) Distribution of τ_f. The red line indicates the fitted line to the single exponential decay function.

waiting time.

To build a replication fork into a Holliday junction structure, it requires three steps – lagging strands displacement, leading strand displacement, and annealing of those two strands. To discover what determines the waiting time, three-color experimental scheme was designed to monitor lagging strand displacement and annealing events simultaneously. As in Figure 4b, one more dye, Cy7 was used. Likewise the Cy3 and Cy5 pair, Cy5 and Cy7 is also a FRET pair, where Cy5 is donor and Cy7 is acceptor. So, for the first time when the fork regression was not occurred, Cy3 and Cy5 pair was in low FRET state and Cy5 and Cy7 pair is in high FRET state. When the fork regression is initiated, the lagging strands displacement will occur, which results that the Cy5 and Cy7 pair will become a low FRET state. After that the annealing event will occur, which results that the Cy3 and Cy5 will become a high FRET state. And then dissociation event will occur and all dye signals will be gone. Figure 5b shows the representative single-molecule trace of the three-color experiment. The waiting time between ATP injection and the annealing time, τ_u, was measured. Surprisingly, τ_u shows clear correlation with τ_f (Figure 5c), which means the rate limiting step would be the lagging strand displacement. Because Mph1 cannot run on the RNA strands [13], and have 3' to 5' directionality [14], each 3' to 5' strand from the junction to the end of the arm was

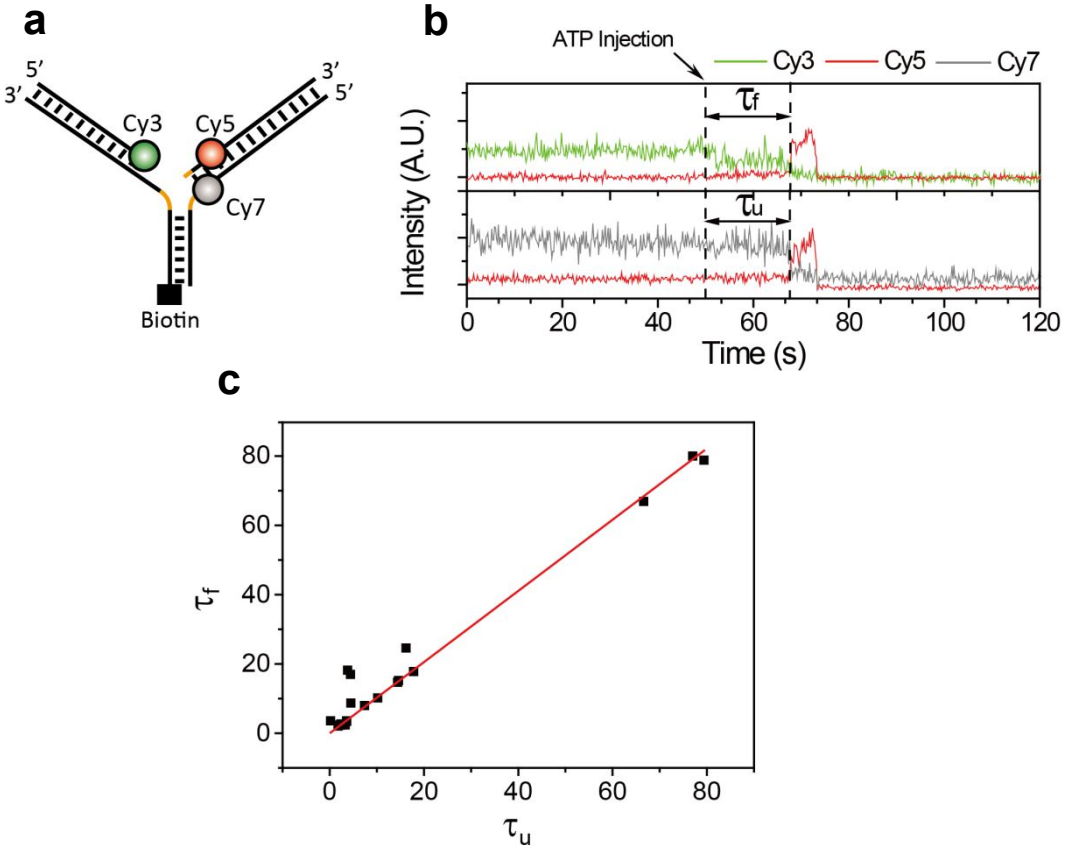

Figure 5

a) DNA sample design for three-color FRET experiment. The Cy3-Cy5 and Cy5-Cy7 pairs are the FRET pairs (donor-acceptor).

b) Representative single-molecule trace of the three-color experimental scheme. As the fork regression starts, the distance between Cy3 and Cy5 become closer (high FRET); that of Cy5 and Cy7 become longer (low FRET).

c) Plot of τ_u vs. τ_f. The red line indicates the linear fitted line. The two dwell times are in close correlation.

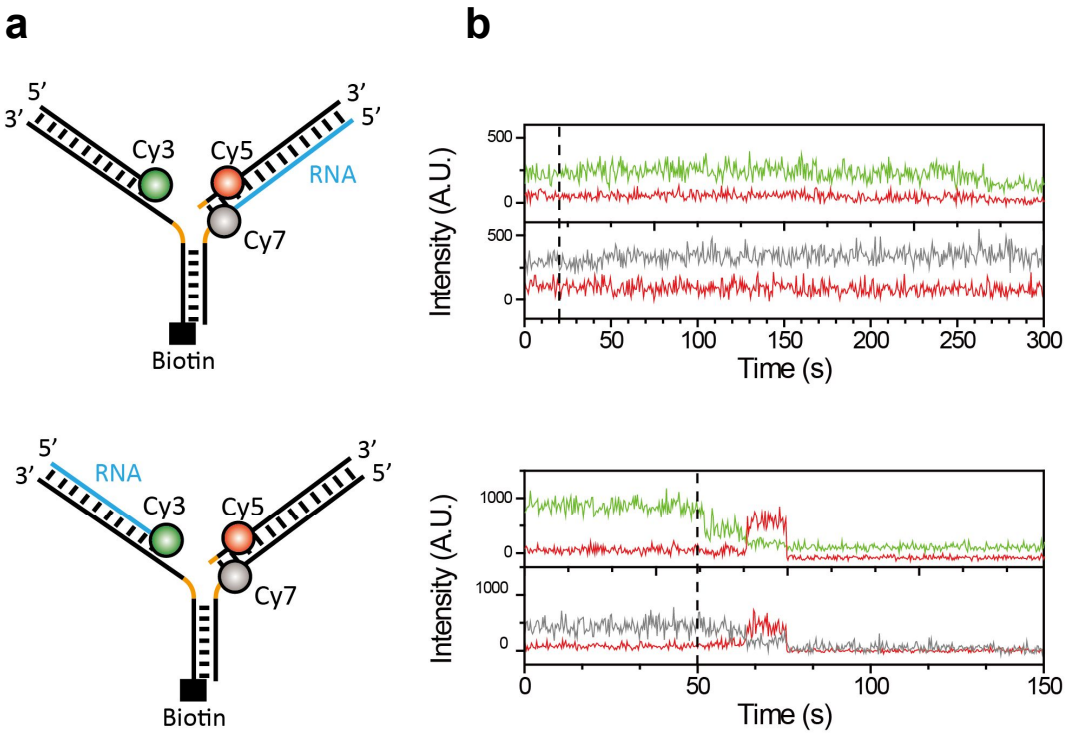

Figure 6

a) The DNA-RNA chimera samples. From the junction side to the end of arm, 3' to 5' strand was replaced to RNA for each arm.

b) Representative trace for the each chimera sample. With lagging arm replaced to the RNA strand (upper one), there was no fork regression activity observed; while the lower one showed fork regression activity.

replaced to RNA strand so that the displacement event of each arm does not occur (Figure 6a). When the lagging arm displacement was suppressed, fork regression does not occur; in contrast to the leading arm was (Figure 6b). So it can be concluded that the rate limiting step is the lagging strand displacement.

3.4. Repetitive Motion of Mph1

In order to observe the behavior of Mph1 when it meets a block while the fork regression is ongoing, DNA sample with 15bp non-homologous pair at the end of the arms was designed (Figure 7b). With the sample, surprisingly, Mph1 turned to backward when it meets the non-homologous region – which results repetitive motion (Figure 7a). This result has never been reported, that's because usual gel electrophoresis cannot observe the real-time progress of fork regression.

Also the high FRET dwell time, τ_r was measured. The distribution of τ_r followed clear single-exponential decay fitted function (Figure 7c). It implies that one rate-limiting step dominates the dwell time, but still the step is unknown. Further studies are required to discover what dominates the dwell time.

Furthermore, to know the effect of the length of the non-homologous region, short non-homologous region was inserted to the DNA sample and the length was varied

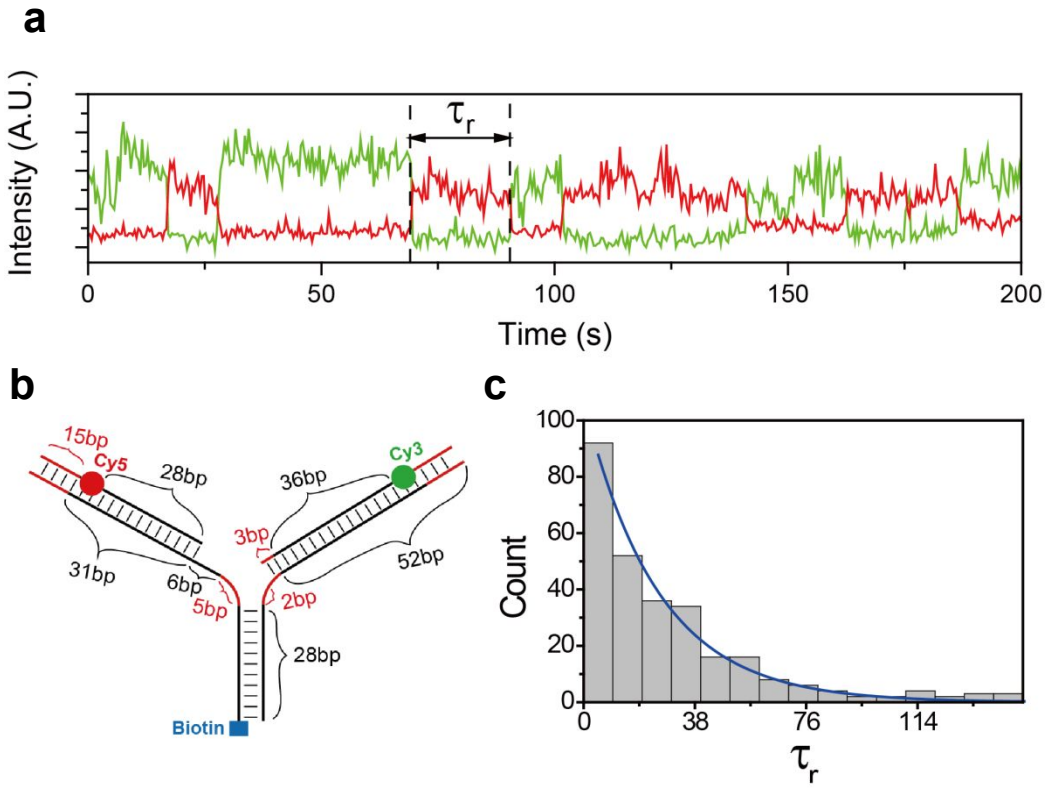

Figure 7

a) Representative single-molecule trace on the sample with 15bp of non-homologous region, which shows repetitive motion of Mph1.

b) DNA sample design with 15bp of non-homologous pairs at the end of arm side.

c) Distribution of τ_r. Blue line indicates the fitted line to the single exponential decay function.

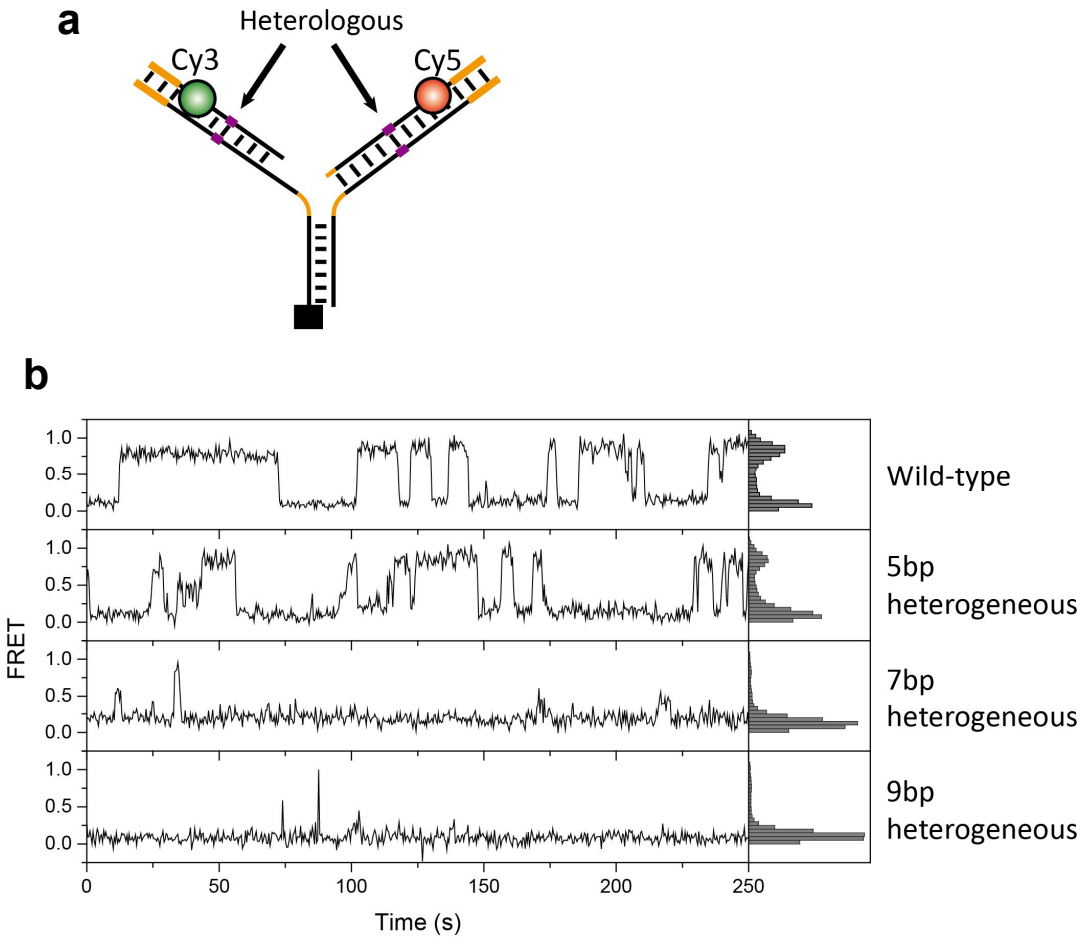

Figure 8

a) DNA scheme with the short non-homologous (heterologous) pair region at the middle of the arm.

b) Representative trace for the wt (15 bp at the end of arm) and 5, 7, and 9 bp at the middle of the arm cases.

through 5, 7, and 9 bp (Figure 8a, 8b).

We found that the critical length of non-homologous region was 5 bp. The representative traces shows the results, Mph1 can run over the short heterogeneous region (under 5 bp), but it returns when the region was more than 5 bp (Figure 8b).

4. Discussion

The behavior of Mph1 is analyzed in single-molecule level for the first time with single-molecule FRET method (Figure 1). As known before, we also found that Mph1 recognizes the structure of replication fork, binds there, and promotes fork regression (Figure 2).

In this paper, we also calculated the speed of fork regression (Figure 3), even looks rather slower than that of the short arm length samples. To know the detail about the contradiction, further studies should be done in the future.

Also we confirmed that Mph1 does not move on RNA strands, and found that Mph1 moves through the lagging-parent strand of replication fork – when the strand is replaced with RNA strand, the fork regression did not occur (Figure 5). In contrast, when the lagging strand displacement did occur, the fork regression successfully occurred even the leading-daughter strand was replaced with RNA

strand. This also means the annealing of two daughter strands occurs naturally after the lagging strand displacement. In addition, we found that the initiation of fork regression is closely related with the lagging strand displacement (Figure 6).

We also tested when Mph1 meets a lesion, which can commonly occur *in vivo*. Surprisingly, we found that Mph1 showed repetitive motion when it meets a non-homologous region while the regression is ongoing (Figure 7). The critical length of the non-homologous region was found, 7 basepairs, which showed that the motion was completely suppressed (Figure 8).

5. Methods

SmFRET experiment was conducted as following. A quartz slide and a cover slip were cleaned up with detergent and the remaining organic residues were burned off in piranha solution, a 3:1 mixture of concentrated sulfuric acid to 30% hydrogen peroxide solution. The cleaned slides were then silanizated with APTMS ((3-aminopropyl)-trimethoxysilane), and then PEGylated with PEG (polyethylene glycol) and biotin-PEG (Laysan Bio) for preventing non-specific binding of proteins on surface. A sample chamber was created by gluing the cover slip and quartz slide with double-sided adhesive tape. 200ug/ml of Straptavidins was injected into the chamber followed by ~100 pM of biotin-attached DNA samples,

so that the injected DNA samples were immobilized by Avidin-Biotin interaction. The imaging buffer, as Gloxy-Glucose oxygen scavenging system and the blinking suppressant Trolox mixture, was made and injected for reducing photobleaching and blinking effects of the dyes. 10nM of Mph1 proteins were mixed within the imaging buffer, and then incubated for about 2 minutes after injection. Free enzymes were washed out by ATP containing imaging buffer solution. The images were taken using a home-built prism-type TIRF microscope at 30 °C. The alternative excitation of Cy3, Cy5 and Cy7 dyes by 532 nm, 633 nm, and 730nm lasers was performed using mechanical shutters for the three-color FRET experiment. The dye signals were collected by a water immersion objective lens (UPlanSApo 60x; Olympus), and filtered through 532 nm, 633 nm, and 730 nm notch filters (NF03-532E-25, NF01-633U-25, and NF03-785E-25 [turned ~43 degree toward incident beam, in order to cut 730 nm range]; Semrock). The fluorescence signals were separated by a dichroic mirrors (635dcxr and 740dcxr; Chroma Technology), and detected by an EMCCD (iXon DV897; Andor).

Chapter 2

Sub-nanometer Resolution Imaging Setup

For overcoming optical diffraction limit, many super-resolution techniques have been developed [15]. Among them, the recently developed two-color sub-nanometer localization method [16] enabled detection of single molecule dynamics by active drift correction and introduction of mapping function. We implemented such a method into our lab, by installing the devices described in the paper and developing a new imaging program which controls the installed devices in real time.

1. Drift Correction in X- and Y-axis

The setup consists of two piezo-mirrors, a dichroic mirror, a pinhole, a partial-reflective mirror, a CCD camera, and lenses (Figure 1a). The image from the microscope is separated into two images by dichroic mirror, and each image is reflected by separate piezo-mirror, and finally makes two image channels on CCD. Besides, a bright pinhole image is merged with the image from microscopy with partial-reflective mirror, and it makes two bright fiducial marks on CCD. And a closed-loop feedback controlling system adjusts the piezo-mirror by locking the

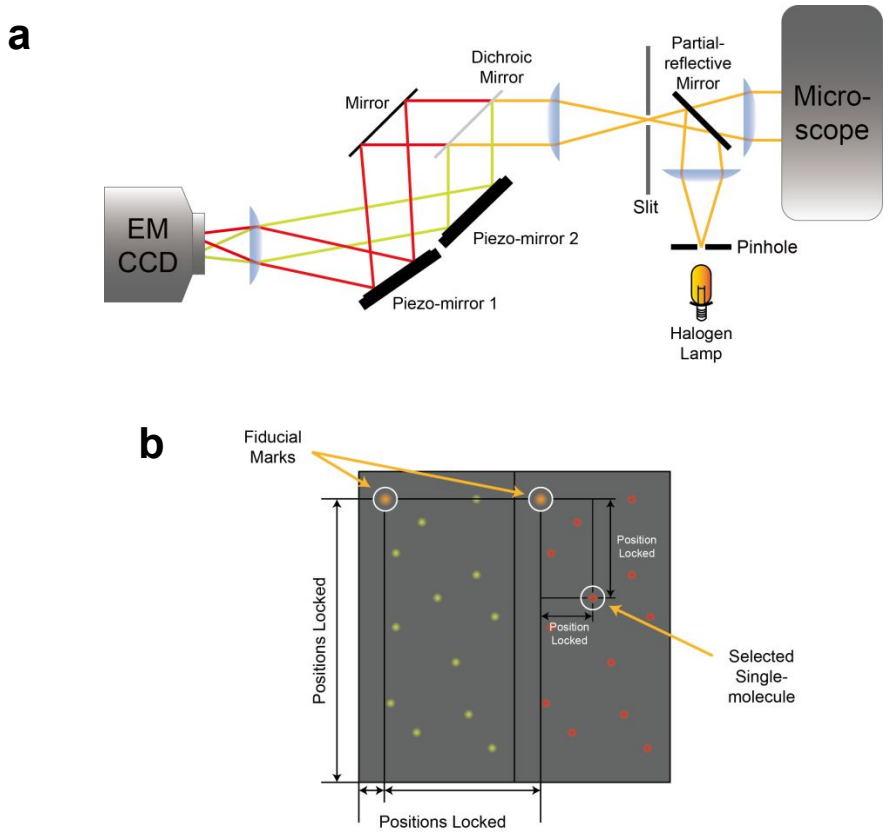

Figure 1

a) The figure shows the aligning of optics used by x- and y-axis drift correction system. The partial reflective mirror reflects pinhole image, and combines it with original single molecule image from microscope. The combined image is separated into two color images by dichroic mirror, and finally approaches on the CCD.

b) Drift correction on x-and y-axis. The absolute positions of fiducial marks and the relative position of the selected single molecule are stabilized on the closed loop.

position of each fiducial mark on CCD, and simultaneously adjusts the piezo-stage so that the distance between the position of one of the single-molecule and the fiducial mark is locked, which results anti-drift behavior in x- and y-axis (Figure 1b). To get the precise position of the fiducial marks and the single molecule, the least square fitted parameter with Gaussian function was used, which is calculated in real time.

2. Drift Correction in Z-axis

In order to correct z-axis drift actively, a separate closed-loop controlling system was developed. The system uses infra-red laser, which is reflected at the surface of cover slip and detected on a quadrant photodiode detector (Figure 2). When the z-axis drift occurred, the pathway of infra-red laser is also changed and detected by the detector. So adjusting the z-axis position of piezo-stage so that the pathway is to be stabilized at the first position corrects the z-axis drift.

3. Program Development

The program was developed with easy user interface, so that anyone can easily start the experiment without extensive learning. The program is a part of single-molecule FRET detection program described in the next chapter.

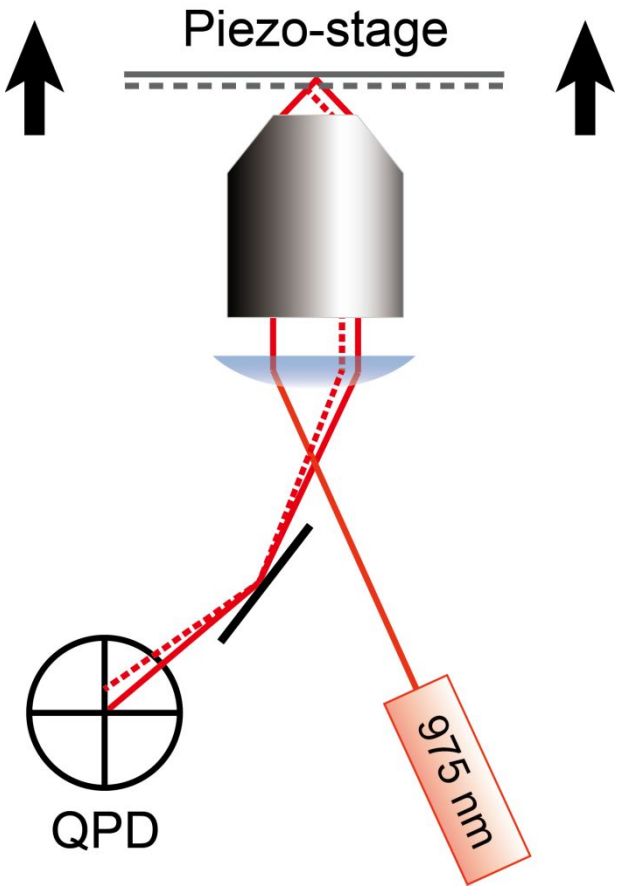

Figure 2

The figure shows Z-axis drift correction. The solid line shows the piezo-stage is at the set-point (the beam reaches to the center of QPD). When the the piezo-stage is located at below set-point, the laser pathway differs (dashed line) and the beam reaches different position of QPD. Then the closed loop algorithm corrects this by moving the piezo-stage upside (arrows on image).

Chapter 3

Development of Single-molecule Imaging Program

For all experiments, custom-made imaging program was developed and used (Figure 1). The program was primarily designed to capture real-time image from EMCCD camera, but also includes ALEX (alternate laser excitation) feature, automatic flow system, and automatic focusing capability [17] for better experimental environment. The program is written in C#, works well on Windows environment. The program will be released in public soon.

1. Unlimited Alternate Laser Excitation (ALEX)

The previous developed programs for single-molecule imaging, can be found on many single-molecule groups' website, does not include ALEX (alternate laser excitation) feature or limited on the laser number. Our lab has developed multi-color FRET setups [18] which requires several lasers in order to excite each dye directly. For example, our lab now even uses 4 lasers simultaneously to achieve direct excitation of Alexa 488, Cy3, Cy5, and Cy7 alternatively.

For the many-color setups can be built in the future, we needed a program can alternatively excites dyes as many as possible. So we built the program which can

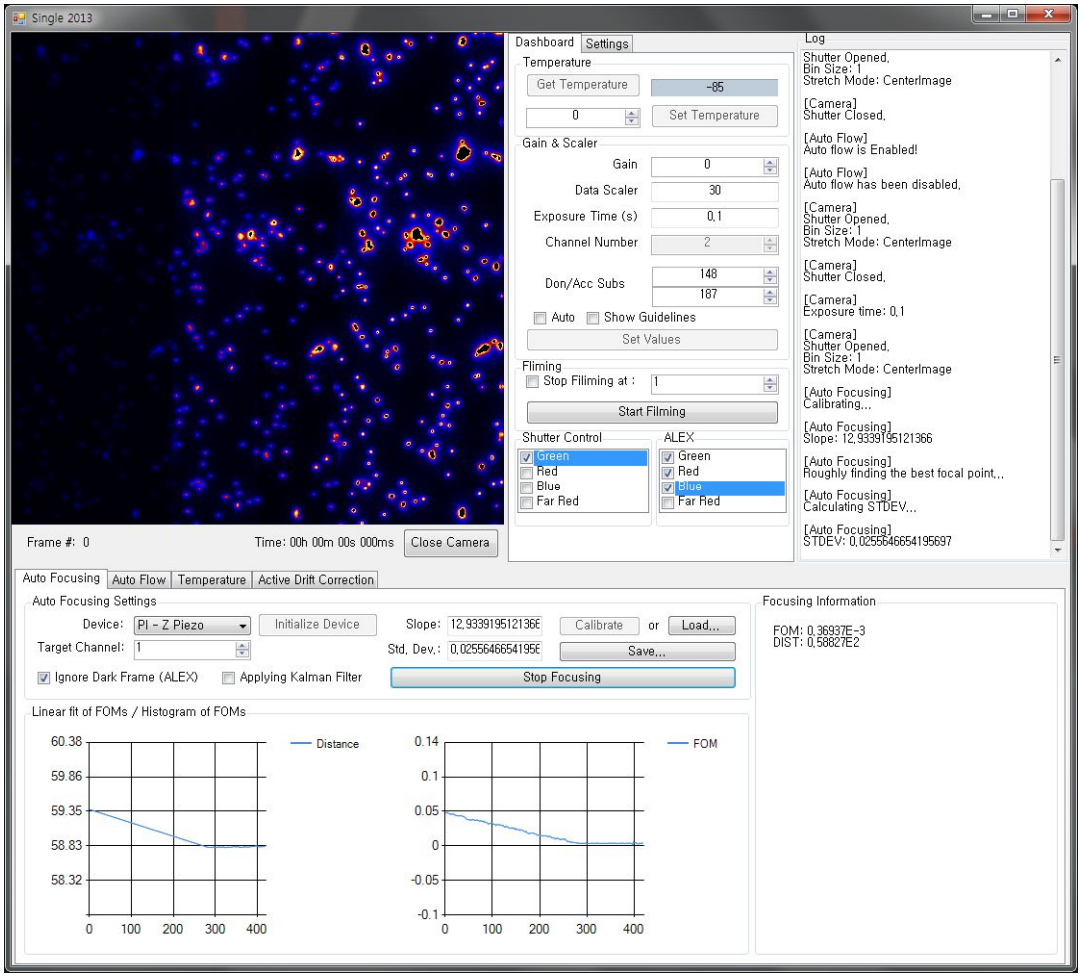

Figure 1

A screenshot of homemade single-molecule imaging program, used for all smFRET experiment described here. By changing the number of lasers in Settings panel, unlimited multi-color shutter control and ALEX is supported. The figure also shows the automatic focusing feature is ongoing.

drive unlimited number of shutters, with unlimited number of ALEX is also capable. In order to drive ALEX, we used National Instrument's PCI-6602 counterboard, which provides high time resolution between the alternate excitations. In general, any National Instrument's counterboard can be used with the program.

2. Automatic Flow System

The program also can control the pump device (currently HARVARD RS-232 pumps and Chemyx USB/RS-232 pumps) via USB or RS232. Because computer sends signal to inject a flow automatically at a given frame number, the injection time of the flow can be stabilized.

From the flow control panel (Figure 2), user can select which pump is used in the experiment. When a user selects a pump, the program automatically retrieves pump's settings and shows them on screen, also enables renewing the setting values into new values. When a user set a frame number and assign flow, the job will be assigned to the right window.

3. Automatic Focusing System

With the prism-type TIRF (total internal reflection fluorescence) setup, the defocusing caused by z-axis drift is very irritating. Our lab developed a real-time

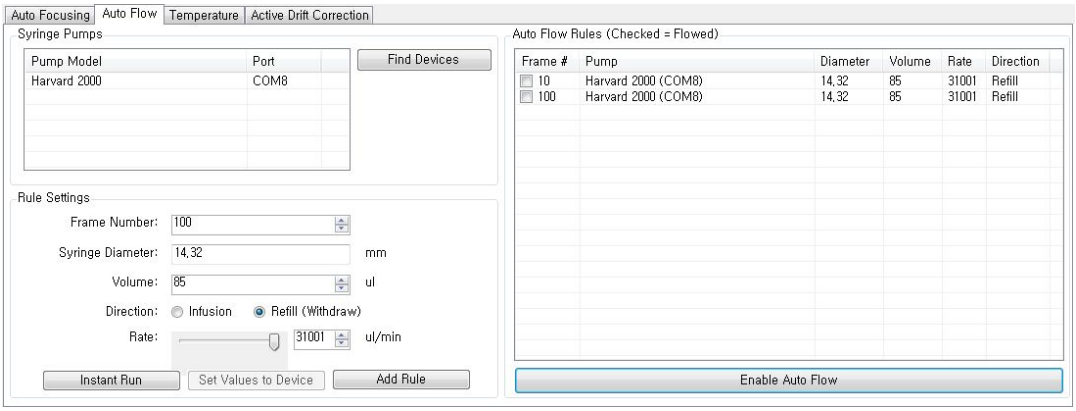

Figure 2

A screenshot of automatic flow control panel. By clicking on 'Find Devices' button, it automatically finds all available pumps connected on system. Selecting a pump will retrieve parameters of the pump, such as syringe diameter, volume, direction, and flow rate. Setting a frame number and clicking 'Add Rule' will register a flow rule, which automatically starts the infusion or refill at a given frame number.

automatic focusing system based on cylindrical lens [17], so that long-time experiments can be done without concerning on the z-axis drift while the imaging is ongoing. Because it does not require many devices but only requires a cylindrical lens on beam path, it can be a cheap and convenient automatic focusing solution for single molecule imaging. It can also be applied to many other single molecule projects with low budget.

4. Active Drift Correction

This feature is a part of sub-nanometer resolution microscopy (described in the previous chapter), to control the closed-loop active drift correction system [16].

The program is in easy interface, just clicking on ‘select’ buttons and click on the desired object on CCD screen will give all required information to the closed-loop algorithm. Anyone can learn how to configure in a minute.

After the feedback correction started working, the information of piezo-mirror angles and the piezo-stage position but also the magnified images of each fiducial marks and selected single molecule are updated in real time, so that one can easily notice the closed loop algorithm is working correctly or not (Figure 3).

The program also provides a way to control piezo-mirrors and piezo-stage manually, with joystick-like easy controlling interface. Also the angle of piezo-mirror and the position of piezo-stage are updated in real time, so that a user can monitor the devices’ real-time information.

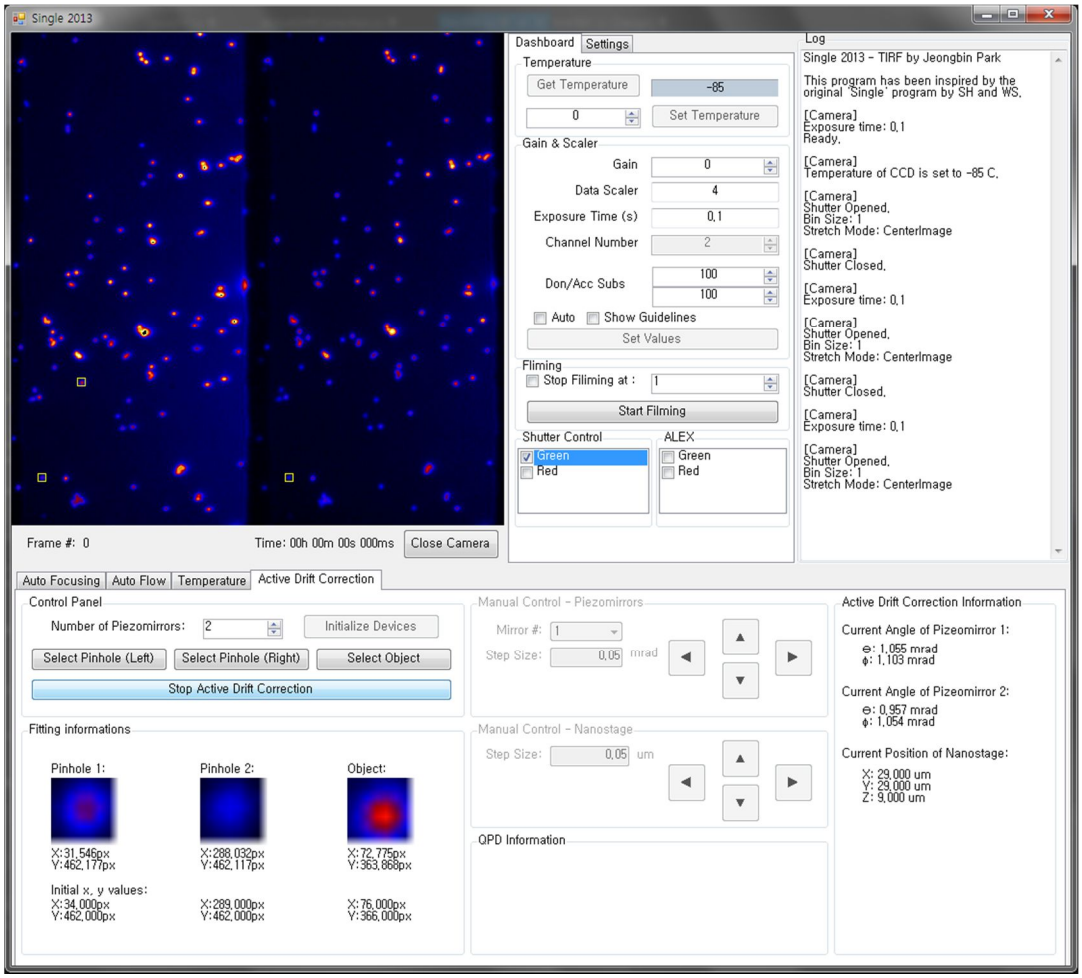

Figure 3

A screenshot of Active drift correction panel, which is taken while the correction is working. Selected pinhole images and single molecule object are noted with yellow square boxes. The magnified images with fitted position information are also shown below, so that one can easily notice the correction status. The devices can also be manually controlled.

Chapter 4

Development of STORM Analysis Program

For other ongoing studies on lab and possible future studies on Mph1, STORM (Stochastic Optical Reconstruction Microscopy) analysis program is developed. The main part of the program is written in OpenCL, an open standard language for parallel programming in heterogeneous environments, enabling operation in diverse platforms such as central processing units (CPUs), graphics processing units (GPUs), and digital signal processors (DSPs). The program is written in Python and Matlab (Mathworks).

We used single-molecule localization microscopy to get super-resolution image, each single molecule image is Gaussian fitted and the precise center position is calculated out as a fit parameter. But usually the labeled flourophores are at a very high density, so it is very difficult to distinguish each of them. So, highly photoswithable dyes are used to overcome the difficult by separating them in the time domain [15]. Finally, super-resolution image is reconstructed by accumulating Gaussian dots with the calculated center position and the photon number of the single molecule spots.

So In order to create the image, the crucial step is Gaussian fitting algorithm, which is usually very slow on personal computers – because although each fitting step is relatively light, but the total number of molecules is huge.

Because the same calculation should be done throughout all single molecule spots, it is the ideal situation to be parallelized. The Gaussian fitting part was rewritten as OpenCL kernel, so that each calculation unit independently carries out the fitting job. Depending on the number of calculation units, for example usual GPUs have several hundreds of calculation units, it can run much faster. We also compared the parallelized algorithm with the same algorithm written in Matlab, the new algorithm was around 40X faster.

OpenCL is supported on various platforms, including many Intel/AMD CPUs and NVidia/AMD graphic cards. Although the program can uses CPU or GPU, but usually GPU is faster (Figure 1). That is because the number of calculation unit is very larger than that of CPU; even the computing power of each calculation unit is weaker. Khronos group provides an extensive list of supported devices (http://www.khronos.org/conformance/adopters/conformant-products/#opencl), so that one can check whether the supported device is installed on system.

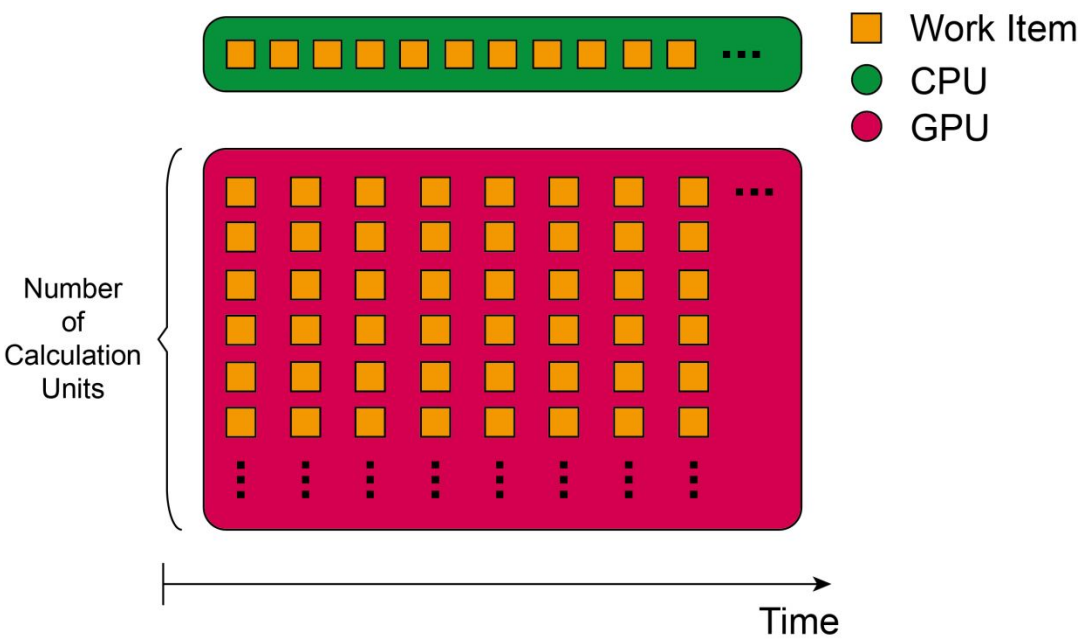

Figure 1

The comparison plot of time vs. CPU and GPU. The green rectangle indicates the calculation on CPU; the red rectangle indicates that on GPU. Although the calculation time per step of GPU can be slower than that of CPU, the number of calculation units of GPU is much more than that of CPU – which results total calculation speed of GPU is much faster.

References

[1] A. J. Deans and S. C. West, Nat. Rev. Cancer **11**, 467 (2011).

[2] A. Ciccia and S. J. Elledge, Mol. Cell **40**, 179 (2010).

[3] W. Lee, R. P. St Onge, M. Proctor, P. Flaherty, M. I. Jordan, A. P. Arkin, R. W. Davis, C. Nislow, and G. Giaever, PLoS Genet. **1**, e24 (2005).

[4] L. J. Niedernhofer, Mol. Cell **25**, 487 (2007).

[5] A. R. Meetei, A. L. Medhurst, C. Ling, Y. Xue, T. R. Singh, P. Bier, J. Steltenpool, S. Stone, I. Dokal, C. G. Mathew, M. Hoatlin, H. Joenje, J. P. de Winter, and W. Wang, Nat. Genet. **37**, 958 (2005).

[6] K. Gari, C. Décaillet, M. Delannoy, L. Wu, and A. Constantinou, Proc. Natl. Acad. Sci. U. S. A. **105**, 16107 (2008).

[7] H. Voss, J. Tamames, C. Teodoru, a Valencia, C. Sensen, S. Wiemann, C. Schwager, J. Zimmermann, C. Sander, and W. Ansorge, Yeast **11**, 61 (1995).

[8] A. C. Douglas, A. M. Smith, S. Sharifpoor, Z. Yan, T. Durbic, L. E. Heisler, A. Y. Lee, O. Ryan, H. Göttert, A. Surendra, D. van Dyk, G. Giaever, C. Boone, C. Nislow, and B. J. Andrews, G3 (Bethesda). **2**, 1279 (2012).

[9] D. L. Daee and K. Myung, Genome Integr. **3**, 7 (2012).

[10] T. a Ward, Z. Dudášová, S. Sarkar, M. R. Bhide, D. Vlasáková, M. Chovanec, and P. J. McHugh, PLoS Genet. **8**, e1002884 (2012).

[11] X.-F. Zheng, R. Prakash, D. Saro, S. Longerich, H. Niu, and P. Sung, DNA Repair (Amst). **10**, 1034 (2011).

[12] R. Roy, S. Hohng, and T. Ha, Nat. Methods **5**, 507 (2008).

[13] J. Banroques, M. Doère, M. Dreyfus, P. Linder, and N. K. Tanner, J. Mol. Biol. **396**, 949 (2010).

[14] R. Prakash, L. Krejci, S. Van Komen, K. Anke Schürer, W. Kramer, and P. Sung, J. Biol. Chem. **280**, 7854 (2005).

[15] B. Huang, M. Bates, and X. Zhuang, Annu. Rev. Biochem. **78**, 993 (2009).

[16] A. Pertsinidis, Y. Zhang, and S. Chu, Nature **466**, 647 (2010).

[17] W. Hwang, S. Bae, and S. Hohng, Opt. Express **20**, 29353 (2012).

[18] S. Hohng, S. Lee, J. Lee, and M. H. Jo, Chem. Soc. Rev. (2013).

국문 초록

Saccharomyces cerevisiae 에서 발견되는 단백질 Mph1은 ATP를 소모하며 DNA 가닥을 푸는 helicase로 3’-5’의 방향성을 지닌다. 이 단백질은 인간에서 발견되는 FANCM과 비슷하게, DNA 가닥 간 공유결합(ICL)으로 인해 DNA가 풀리지 못하여 복제가 중단된 DNA 복제 포크를 복원하는데 한 역할을 하는 것으로 알려져 있다. 본 연구에서는 이러한 복구과정이 어떻게 일어나는지 알아보기 위하여, 단분자 FRET법으로 중단된 복제 포크를 되돌리는 Fork Regression 과정을 관찰하였다. 본 연구를 통해 Chicken-foot 구조의 형성과 지연 가닥이 풀리는 과정간 큰 연관성이 있는 것을 발견하였다. 또한 DNA 가닥이 서로 일치하지 않아 Fork Regression이 일어나지 못하는 상황에 처한 경우, Mph1이 앞 뒤로 왕복하여 움직인다는 것 또한 발견하였다.

핵심어: Mph1, DEAH-box DNA Helicase, DNA 복제, Fork Regression, ICL 복구, 단일분자 FRET

학번: 2012-20361